



HAL
open science

Broadband vibration damping of a non-periodic plate by piezoelectric coupling to its electrical analogue

Robin Darleux, Boris Lossouarn, Jean-François Deü

► To cite this version:

Robin Darleux, Boris Lossouarn, Jean-François Deü. Broadband vibration damping of a non-periodic plate by piezoelectric coupling to its electrical analogue. 9th ECCOMAS Thematic Conference on Smart Structures and Materials, SMART 2019, Jul 2019, Paris, France. hal-02237890

HAL Id: hal-02237890

<https://hal.science/hal-02237890>

Submitted on 31 Jul 2020

HAL is a multi-disciplinary open access archive for the deposit and dissemination of scientific research documents, whether they are published or not. The documents may come from teaching and research institutions in France or abroad, or from public or private research centers.

L'archive ouverte pluridisciplinaire **HAL**, est destinée au dépôt et à la diffusion de documents scientifiques de niveau recherche, publiés ou non, émanant des établissements d'enseignement et de recherche français ou étrangers, des laboratoires publics ou privés.

BROADBAND VIBRATION DAMPING OF A NON-PERIODIC PLATE BY PIEZOELECTRIC COUPLING TO ITS ELECTRICAL ANALOGUE

R. DARLEUX*, B. LOSSOUARN[†] AND J.-F. DEÜ[†]

* [†] Laboratoire de Mécanique des Structures et des Systèmes Couplés (LMSSC)

Conservatoire national des arts et métiers (Cnam)

292 rue Saint-Martin, 75003 Paris, France

e-mail: robin.darleux@lecnam.net, web page: <http://www.lmssc.cnam.fr>

Key words: Vibration control, Multimodal damping, Piezoelectric coupling, Direct electromechanical analogy, Finite Element model

Abstract. Several solutions for multimodal vibration damping of thin mechanical structures based on piezoelectric coupling have been developed over the years. Among them, piezoelectric network damping consists in using piezoelectric transducers to couple a structure to an electrical network, where the transferred electrical energy can be dissipated. In particular, the effectiveness of coupling rods, beams and plates to networks which are their electrical analogues has been proven. This work is the first step going towards more complex structures. After defining and experimentally validating a new electrical analogue of a simply-supported plate, the study is extended to the damping of a non-periodic plate. Experiments show that in this case, a broadband damping is achieved once the piezoelectric transducers are coupled to an adequate analogous network. A finite element model of the structure coupled to its analogous network is concurrently developed and validated.

1 INTRODUCTION

Single mode damping of mechanical vibrations using the piezoelectric coupling goes back to the 1990s, when the resonant shunt was described by Hagood and Von Flotow [1]. The concept of piezoelectric damping has then been extended to multimodal damping. Some passive solutions consider connecting a multi-branch shunt to a piezoelectric transducer [2, 3]. While adding only one piezoelectric transducer to the structure is barely intrusive, its position and dimensions cannot simultaneously maximize the electromechanical coupling for all modes [4]. For these reasons, the damping performance might be limited. Other solutions include several independent piezoelectric transducers, each one being shunted in order to damp one mode of the structure. However, the resulting electromechanical coupling coefficients are inferior to the ones that would be induced by interconnecting all piezoelectric transducers.

In the early 2000s, the idea of interconnecting piezoelectric transducers with electrical components emerged. The concept of achieving broadband damping by coupling a structure to an electrical network was first proposed by Vidoli and dell'Isola [5]. Meanwhile, the electrical analogues of mechanical structures, as defined by MacNeal and Bescoter [6, 7] in the early 1950s, have been revived for multimodal vibration attenuation purposes [8]. As a consequence, piezoelectric network damping of plates has been studied [9, 10], and implemented recently [11, 12]. The next objective is to study the multimodal damping of complex structures coupled to their electrical analogues. To study the case of a non-periodic plate is considered as the first step towards this goal.

Moreover, a predictive model of the dynamics of the coupled system would be helpful to investigate the limits of the analogy between the structure and its electrical analogue. It could also be used to find the resistive components to add to the network to get an optimized damping performance. To develop such a model, the work of Thomas et al. [13] concerning a structure covered by thin piezoelectric patches is taken as the starting point.

Section 2 explains how to define a plate electrical analogue. It is applied to a practical setup of a simply-supported plate, and validated by comparing mechanical and electrical measurements. In section 3, we develop a finite element model of the plate coupled to its electrical analogue. The model is validated by comparing simulated and experimental results. Finally, the case of a non-periodic plate is addressed in section 4. A mass is added on the plate to break its symmetry. The designed electrical analogue is experimentally validated and passive broadband damping is still achieved.

2 PLATE ELECTRICAL ANALOGUE

In this first section, the direct electromechanical analogy is applied to a finite difference model of a square plate. The resulting set of equations can be represented by an electrical circuit with lumped elements. The electrical analogue of a square plate is then assembled to produce a plate electrical analogue, which is implemented and validated. The validation is conducted by comparing the operational shapes of the plate and of its electrical analogue.

2.1 Finite difference model of a square plate

The motion of a plate of thickness h , mass density ρ and bending stiffness D is described by the Kirchhoff-Love plate theory, so that

$$-D \left(\frac{\partial^4 w}{\partial x^4} + 2 \frac{\partial^4 w}{\partial x^2 \partial y^2} + \frac{\partial^4 w}{\partial y^4} \right) = \rho h \ddot{w}. \quad (1)$$

In harmonic motion at angular frequency Ω , Eq. (1) is equivalent to

$$\begin{cases} \frac{\partial Q_x}{\partial x} + \frac{\partial Q_y}{\partial y} = -\frac{m}{a} \Omega^2 w \\ M = aD \left(\frac{\partial \theta_x}{\partial x} + \frac{\partial \theta_y}{\partial y} \right) \end{cases} \quad \text{where} \quad Q_x = -\frac{\partial M}{\partial x}, \quad Q_y = -\frac{\partial M}{\partial y}, \quad \theta_x = \frac{\partial w}{\partial x}, \quad \theta_y = \frac{\partial w}{\partial y}. \quad (2)$$

With these notations, w is the displacement in the direction normal to the plate, a is the side of the square plate, $m = \rho h a^2$ is its mass, Q_x and Q_y are the shear forces in the plate, θ_x and θ_y are the angles along the principal directions, and M is a linear combination of the bending moments along the x and y directions defined by Timoshenko in [14]. A finite difference pattern, as represented in Figure 1, is then applied to the plate model. The resulting system of equations obtained from Eqs. (2) is expressed by

$$\begin{cases} Q_T - Q_B + Q_R - Q_L = -m\Omega^2 w_I \\ M_I = D(\theta_T - \theta_B + \theta_R - \theta_L) \end{cases}, \quad \frac{a}{2} \begin{pmatrix} -Q_B \\ -Q_L \\ Q_R \\ Q_T \end{pmatrix} = \begin{pmatrix} M_I - M_B \\ M_I - M_L \\ M_I - M_R \\ M_I - M_T \end{pmatrix}, \quad \frac{a}{2} \begin{pmatrix} \theta_B \\ \theta_L \\ -\theta_R \\ -\theta_T \end{pmatrix} = \begin{pmatrix} w_I - w_B \\ w_I - w_L \\ w_I - w_R \\ w_I - w_T \end{pmatrix} \quad (3)$$

2.2 Design of the plate electrical analogue

The direct electromechanical analogy, such as presented by Bloch in [15], allows the representation of mechanical structures with passive electrical components. In the case here studied, this means that the electrical analogue of a square plate is defined by replacing mechanical quantities in Eqs. (3) by electrical quantities, according to the analogy in Table 1. The first two equations in the system of Eqs. (3) can

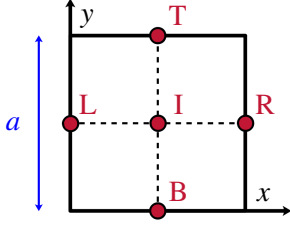


Figure 1: Discretization grid, where I, B, L, R, T refer to the central, bottom, left, right and top positions, respectively

Mechanical quantities		Electrical quantities
Force Q		Voltage V_w
Moment M		Voltage V_θ
Linear velocity \dot{w}		Electrical current \dot{q}_w
Angular velocity $\dot{\theta}$	\iff	Electrical current \dot{q}_θ
Compliance $1/D$		Capacitance C
Mass m		Inductance L
Lever arm $a/2$		Transformer ratio $\hat{a}/2$

Table 1: Direct electromechanical analogy

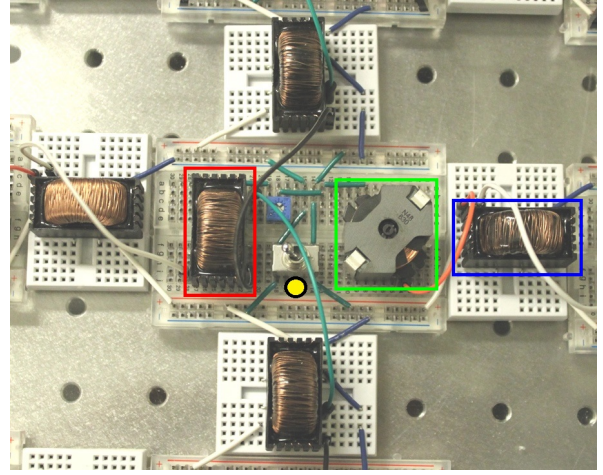
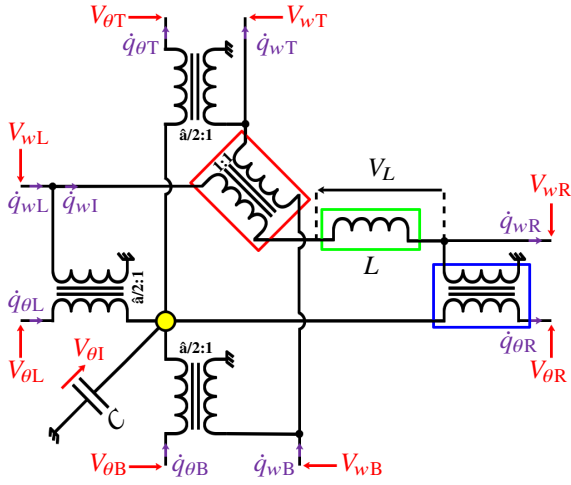


Figure 2: Scheme and picture of the electrical analogue of a square plate, which highlight the central transformer in red, a side transformer in blue, the inductance in green, and the capacitance connection in yellow

be understood as constitutive equations of an ideal inductor of inductance m and an ideal capacitor of capacitance $1/D$. The remaining equations can be interpreted as constitutive equations of transformers of ratio $a/2$. Hence, the Figure 2 represents the unit cell of the plate electrical analogue. The electrical analogue of a rectangle plate can then be defined by assembling this unit cell along the x and y directions.

Moreover, the boundary conditions of the plate should be reproduced in the electrical network. In particular, the simply-supported and clamped edges have direct equivalent electrical connections. Indeed, if for example the left edge of the unit cell is a boundary, then the simply-supported condition is equivalent to command that $V_{\theta L} = 0$ and $\dot{q}_{wL} = 0$, while the clamped condition is equivalent to command $\dot{q}_{\theta L} = 0$ and $\dot{q}_{wL} = 0$ [12].

Finally, the electrical components should be tuned so that the natural frequencies of the network are equal to the natural frequencies of the plate [11]. This ensures identical bending wave propagation properties in the two media. In this case, the modal coupling condition is

$$\frac{1}{a^2} \frac{D}{m} = \frac{1}{\hat{a}^2} \frac{1}{LC}. \quad (4)$$

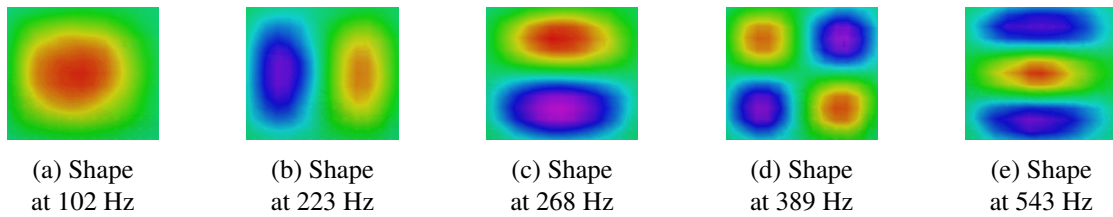


Figure 3: Measurement of five operational deflection shapes of the plate

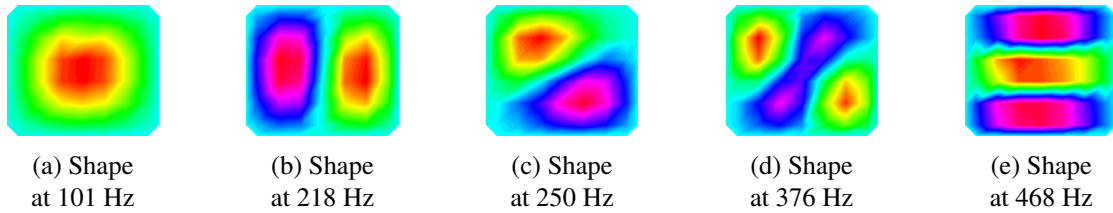


Figure 4: Measurement of five operational electrical current shapes in the network

2.3 Validation of the plate electrical analogue

The considered setup is a simply-supported aluminium plate of dimensions $420 \times 360 \times 3$ mm³. It is periodically covered with 42 square piezoelectric patches of dimensions $50 \times 50 \times 0.5$ mm³. The objective is to develop the electrical analogue of this structure. Hence, a network made of 42 identical unit cells has been assembled. The structure and its analogous network are shown in Figure 7, while one unit cell is shown in Figure 2. A way to validate the plate electrical analogue is to compare its operational electrical current shapes to the deflection shapes of the plate.

Since the network should be tested alone for validation, the piezoelectric patches are replaced by ceramic capacitors which have a nominal capacitance of 145 nF. Then, following the method described in [16], the inductors are made by winding conductive wire around a RM10 core of N48 ferrite material from Epcos TDK. The nominal inductance and series resistance of the produced inductors are $L = 244$ mH and $R_{sL} = 13.7$ Ω . Finally, the ratio of the transformers is $\hat{a} = 4$, and their nominal series resistance is 16.8 Ω when used with a 1:1 ratio. An inductor and several transformers are pictured in Figure 2.

By analogy with an exciting external force, an external voltage is applied between two unit cells of the network. The voltage V_{ex} is applied through an isolation transformer of ratio k , such as represented in Figure 5. At the same time, the voltage drop V_L across each inductor of the network is measured. Dividing V_L by the impedance $R_{sL} + jL\Omega$ leads to the electrical current \dot{q}_{wI} flowing through each inductor. As a consequence, plotting the shapes of \dot{q}_{wI}/kV_{ex} is equivalent to plotting the operational deflection shapes of a plate excited by a point load. Several operational deflection shapes of the plate have been measured using a laser vibrometer and are represented in Figure 3. These can be compared to the operational current shapes in Figure 4. Plotted shapes look alike, even though some shapes are slightly different, such as in Figure 3c and Figure 4c. This can be explained by the heavy damping due to resistive components in the electrical network. Hence, operational electrical current shapes may spill over onto each other. It is the case in Figure 4c, where the measured current distribution looks like a combination of modes (1,2) and (2,1). For this reason, further investigations could include the experimental modal analysis to separate the contributions of modes. Anyway, comparing operational shapes offers a first validation of the plate electrical analogue.

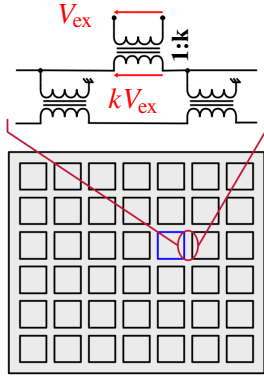


Figure 5: Schematic representation of the excitation setup for the measurement of network modes

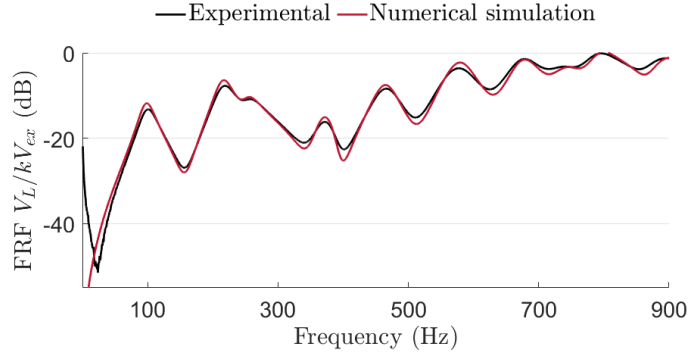


Figure 6: Experimental and simulated FRFs, with V_L measured across the inductor of the unit cell highlighted in blue in Figure 5

Furthermore, we developed a lumped model of the entire network. The unit cells, as schematised in Figure 2, are put together following an assembly process. The boundary conditions are then set such as described in section 2.2. The numerical Frequency Response Functions (FRFs) V_L/kV_{ex} can thus be compared to measurements. As an example, a comparison is plotted in Figure 6 for V_L measured in the unit cell highlighted in blue in Figure 5. The simulated FRFs fit with the the measured ones. The remaining differences can be reduced by taking other parasitic elements of the transformers into account, such as the magnetizing branch and the winding capacitance. These kinds of refined models are not presented for the sake of conciseness, and because the correlation between the proposed model and experiments is considered good enough to validate the concept of the plate electrical analogue.

3 FINITE ELEMENT MODEL OF A STRUCTURE COUPLED TO ITS ELECTRICAL ANALOGUE

The main steps to model the dynamics of a mechanical structure covered by piezoelectric patches are recalled. Then, the effect of the interconnections between patches via an electrical network is accounted for. The simulated results are finally compared to experiments in order to validate the approach.

3.1 Finite element formulation

To model the vibrations of a continuous medium covered with piezoelectric patches, we follow the method described by Thomas et al. in [13]. Though all equations are not detailed in this paper, the main steps to develop a finite element model of the structure are recalled.

The electric field is denoted \mathbf{E} . The electric displacement is denoted \mathbf{D} . Using the Voigt notation, the linearized stress and strain vectors are respectively denoted $\boldsymbol{\sigma}$ and $\boldsymbol{\varepsilon}$. The electro-mechanical constitutive equations linking these quantities are

$$\begin{aligned}\boldsymbol{\sigma} &= \mathbf{C}^E \boldsymbol{\varepsilon} - \mathbf{e}^T \mathbf{E}, \\ \mathbf{D} &= \mathbf{e} \boldsymbol{\varepsilon} + \boldsymbol{\epsilon}^E \mathbf{E},\end{aligned}\quad (5)$$

where \mathbf{C}^E is the matrix of elastic coefficients at constant electric field, \mathbf{e} is the matrix of piezoelectric coefficients, and $\boldsymbol{\epsilon}^E$ is the matrix of dielectric permittivities at constant strain. The structure is modelled as an isotropic homogeneous linear elastic medium in which $\mathbf{e} = \mathbf{0}$. Furthermore, the piezoelectric transducers exhibit transverse isotropic properties and are polarized in their transverse directions $\mathbf{n}^{(i)}$. The

patches thickness's, denoted $h^{(j)}$, are considered small when compared to their longitudinal dimensions. Hence, the electrical field $\mathbf{E}^{(j)}$ in the j -th piezoelectric patch is supposed uniform and normal to the electrodes. It can be expressed as a function of the potential difference $V^{(j)}$ between electrodes of each patch:

$$\mathbf{E}^{(j)} = -\frac{V^{(j)}}{h^{(j)}}\mathbf{n}^{(j)}. \quad (6)$$

To derive the mechanical equation of the variational formulation, the elastodynamic equation, in which prescribed body forces are neglected, is considered. To derive the electrical equation, it is Gauss's law involving no free charges which is considered. These equations are then multiplied by test functions and integrated over the entire volume of the structure. The prescribed surface forces and free charge densities are taken into account as boundary conditions. Then, the constitutive equations of the medium are applied to get the variational formulation in terms of displacement \mathbf{u} and electric potential $V^{(j)}$.

The equations of the variational formulation are then discretized. Following an assembly process, we obtain a finite element formulation of the coupled problem:

$$\begin{pmatrix} \mathbf{M}_m & \mathbf{0} \\ \mathbf{0} & \mathbf{0} \end{pmatrix} \begin{pmatrix} \ddot{\mathbf{U}} \\ \ddot{\mathbf{V}} \end{pmatrix} + \begin{pmatrix} \mathbf{K}_m & \mathbf{K}_c \\ -\mathbf{K}_c^T & \mathbf{K}_e^{-1} \end{pmatrix} \begin{pmatrix} \mathbf{U} \\ \mathbf{V} \end{pmatrix} = \begin{pmatrix} \mathbf{F} \\ \mathbf{Q} \end{pmatrix}, \quad (7)$$

where \mathbf{U} contains the nodal values of the displacement field \mathbf{u} and \mathbf{V} contains the voltage values ($V^{(1)}, \dots, V^{(P)}$) on the upper electrodes of the piezoelectric patches. \mathbf{F} represents the external mechanical forces applied to the structure, while \mathbf{Q} are the electrical charges on the upper electrodes of the piezoelectric patches. \mathbf{K}_c is the coupling matrix, and \mathbf{M}_m and \mathbf{K}_m are the mass and mechanical stiffness matrices. \mathbf{K}_e is a diagonal matrix in which the j -th term is the inverse of the blocked piezoelectric capacitance $C^{(j)}$ of the j -th patch, which is

$$C^{(j)} = \frac{\epsilon_{33}^{\mathcal{E}} S^{(j)}}{h^{(j)}}, \quad (8)$$

where $S^{(j)}$ is the j -th patch surface and $\epsilon_{33}^{\mathcal{E}}$ is the transverse permittivity of a piezoelectric medium with no strain. In the case of plate bending, this quantity can be estimated with materials constants. More details are available in [11].

3.2 Coupling of a structure to its electrical analogue

The piezoelectric patches bound to the structure are interconnected via the plate electrical analogue. Hence, using the notations in Figure 2, \mathbf{V} contains in fact the voltage values ($V_{\theta I}^{(1)}, \dots, V_{\theta I}^{(P)}$), while the j -th element of \mathbf{Q} is equal to the charge $q_{\theta B}^{(j)} - q_{\theta T}^{(j)} + q_{\theta L}^{(j)} - q_{\theta R}^{(j)}$ flowing through the capacitance $C^{(j)}$. As a consequence, the network is a passive electrical controller that commands a relationship between \mathbf{V} and \mathbf{Q} . We choose to express these vectors in terms of the 42 electrical charges q_{wI} flowing through the inductors of the network, whose values are contained in the vector \mathbf{Q}_w . Using a symbolic solver, we obtained these relations:

$$\begin{aligned} \mathbf{V} &= -\left(\mathbf{M}_e \ddot{\mathbf{Q}}_w + \mathbf{D}_e \dot{\mathbf{Q}}_w\right), \\ \mathbf{Q} &= \mathbf{P} \mathbf{Q}_w, \end{aligned} \quad (9)$$

which leads to the finite element formulation of the mechanical structure coupled to its electrical analogue:

$$\begin{pmatrix} \mathbf{M}_m & \mathbf{0} \\ \mathbf{0} & \mathbf{M}_e \end{pmatrix} \begin{pmatrix} \ddot{\mathbf{U}} \\ \ddot{\mathbf{Q}}_w \end{pmatrix} + \begin{pmatrix} \mathbf{0} & \mathbf{0} \\ \mathbf{0} & \mathbf{D}_e \end{pmatrix} \begin{pmatrix} \dot{\mathbf{U}} \\ \dot{\mathbf{Q}}_w \end{pmatrix} + \begin{pmatrix} \mathbf{K}_m + \mathbf{K}_c \mathbf{K}_e \mathbf{K}_c^T & \mathbf{K}_c \mathbf{K}_e \mathbf{P} \\ \mathbf{K}_e \mathbf{K}_c^T & \mathbf{K}_e \mathbf{P} \end{pmatrix} \begin{pmatrix} \mathbf{U} \\ \mathbf{Q}_w \end{pmatrix} = \begin{pmatrix} \mathbf{F} \\ \mathbf{0} \end{pmatrix}. \quad (10)$$

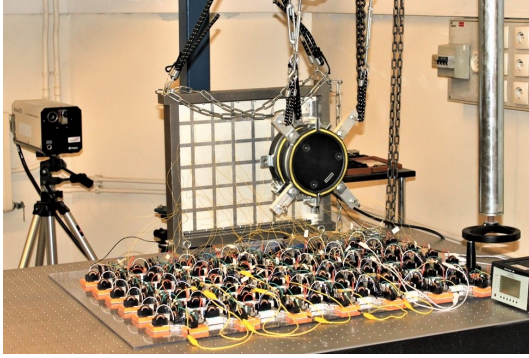


Figure 7: Setup including the plate covered with piezoelectric transducers, a shaker, a laser vibrometer and the plate electrical analogue

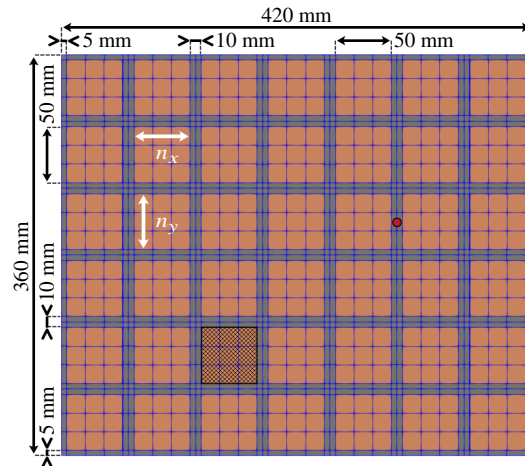


Figure 8: Meshing of the mechanical structure and location (in red) of both the excitation and the velocity measurement

The expressions of the electrical "mass" matrix \mathbf{M}_e , the electrical damping matrix \mathbf{D}_e , and the transfer matrix \mathbf{P} are not detailed in this work for the sake of conciseness. We just precise these three matrices depend on the transformer ratio \hat{a} . Moreover, \mathbf{M}_e is a function of the inductance value L , while \mathbf{D}_e is a function of the series resistance of the inductors R_{sL} and the series resistance of the transformers.

3.3 Validation of the finite element model

Numerical simulations are compared to practical measurements to validate the finite element model developed in the previous sections. The experimental setup is presented in Figure 7. The simply-supported plate periodically covered with piezoelectric patches is suspended. A shaker applies a point load and a force transducer measures it. A laser vibrometer measures the velocity on the other side of the plate. The red marker in Figure 8 represents the location of both the excitation and the velocity measurement. Moreover, the upper electrodes of the patches are either connected to the ground or to the network thanks to switches, which can be spotted in Figure 2.

The structure is modelled with 20-node hexahedral elements. Both the plate and the piezoelectric patches are meshed with one element in depth. In the other directions, the piezoelectric patches as well as the plate beneath them are meshed with $n_x \times n_y$ elements. Taking $n_x = n_y = 3$ leads to converged values for natural frequencies of the undamped structure up to 1 kHz. As a consequence, the Figure 8 represents the mesh used to obtain all the following numerical results.

The plate is made of duralumin. Its Poisson's ratio and density are respectively set at 0.346 and 2800 kg/m^3 . Its Young's modulus is set at 68.8 GPa to adjust the eleventh natural frequency of the plate calculated with short-circuited piezoelectric patches to the corresponding resonances in the experimental measurement. This corresponds to the last peak before 900 Hz as plotted in Figure 9. The piezoelectric patches are made of the PIC 153 PZT material. The coefficients of matrices in Eq. (5) are either taken from manufacturer's data when available, or extrapolated from datasheets of other PZT materials.

The case of short-circuited patches is simulated by imposing all voltage values in \mathbf{V} to ground potential in Eq. (7). The plotted results in Figure 9 show that the numerical simulation forecasts the dynamics of the structure up to 900 Hz rather well. Moreover, the remaining differences between numerical and experimental results could be reduced. First of all, the plate is linked to a rigid frame via thin supports.

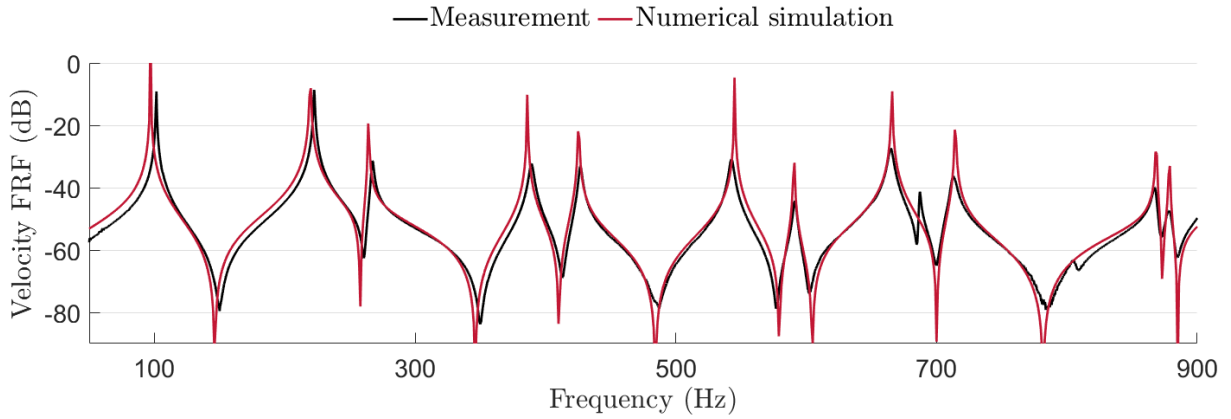


Figure 9: Experimental and simulated FRFs with short-circuited piezoelectric patches

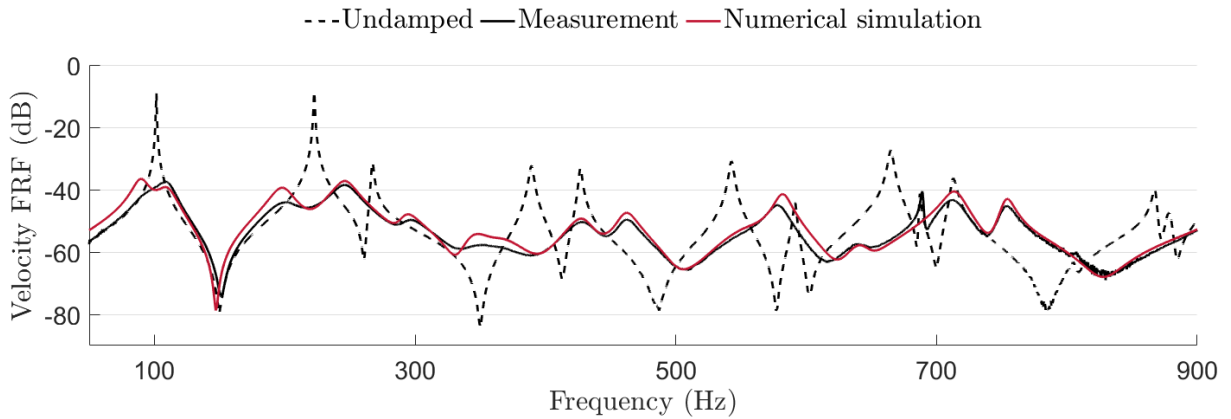


Figure 10: Experimental and simulated FRFs when the plate is coupled to its electrical analogue

The plate is the only part of the assembly that is modelled. Since the peak at 687 Hz is a frame mode, it can not be predicted. Furthermore, the gaps between the first simulated and measured peaks can be attributed to the non-ideal experimental boundary conditions. This has been explained by Robin et al., who designed a first version of the setup in [17]. Finally, the structural damping has been neglected, which explains the amplitude differences at resonances.

The case of the structure being coupled to its passive electrical analogue is then considered. As seen in Figure 10, a broadband vibration damping is achieved. Meanwhile, the frame mode at 687 Hz is barely affected by the connection to the network, which was expected. Besides, the model in Eq. (10) is able to predict the dynamics of the structure coupled to its electrical analogue. The modelling limits highlighted in Figure 9 remain true in this case. Hence, this model could be used to find the optimal resistive components to be added to the network in order to optimize the damping performance.

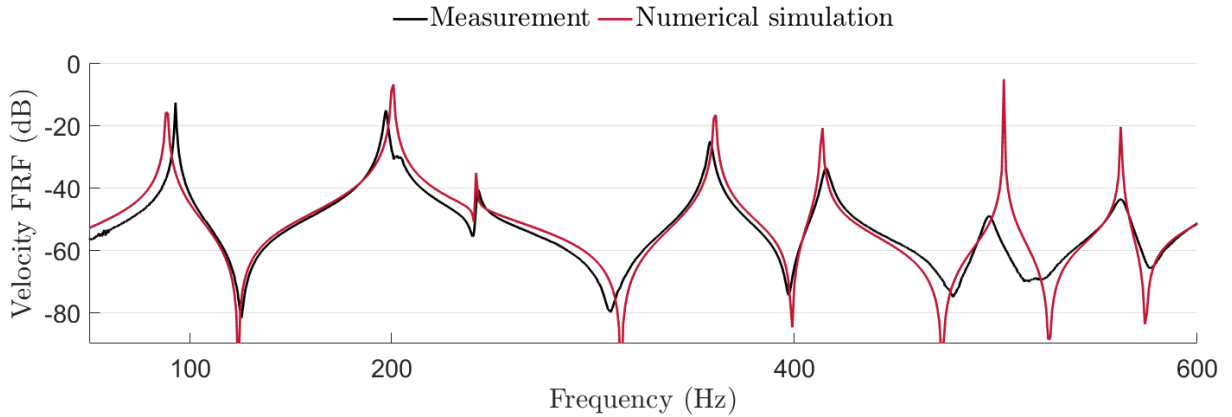


Figure 11: Experimental and simulated FRFs with short-circuited piezoelectric patches and an added mass

4 BROADBAND VIBRATION DAMPING OF A NON-PERIODIC PLATE

In this section, the broadband damping achieved by coupling a structure to its electrical analogue is extended to the case of a non-periodic plate. A mass is locally added on the plate, and its influence on the dynamics of the system is modelled. We then define the non-periodic plate electrical analogue and verify that the first few modes of the structure are significantly damped.

4.1 Non-periodic plate electrical analogue and validation

Designing the electrical analogue of a non-periodic plate is the first step towards more complex structures. As a consequence, we decided to add a mass which is a 22 mm thick, 40 mm diameter cylindrical rod of 207 g. This mass is added on the side of the plate which is not covered by piezoelectric patches, on the hatched position in Figure 8.

The mass is added in the finite element model as well, in the form of a 22 mm thick patch covering the same surface as a piezoelectric patch. Its Young modulus is set at 325 MPa. This way, the seventh simulated natural frequency of the plate with short-circuited patches is adjusted to the seventh peak on the measured FRF. The correlation between numerical and experimental results in this case is shown in Figure 11. When compared to the results in Figure 9, one can notice that the natural frequencies of the plate have been lowered, that the contact with the added mass induces damping in the measured FRF, and that a frame mode at 203 Hz is now excited. Since the structural damping and the frame are not taken into account, their effects are not foreseen by our model. The simulated FRF fits quite well with the measured one nonetheless.

The non-periodic plate here considered is obtained by locally adding some mass and some stiffness to the structure. To get its electrical analogue, the first natural frequency of the electrical network should be adjusted to the first natural frequency of the non-periodic plate. The first simulated resonance in Figure 11 is used as a reference value for the structure. In other words, Eq. (4) should remain true, while a and \hat{a} have set values and D and m are locally modified. Thus, one should modify the product of the capacitance C by the inductance L of the corresponding unit cell of the network. Not to deteriorate the electromechanical coupling [18], only L is modified to adjust the first natural frequency of the electrical network. The calculations, which are not detailed here, show in this case that the initial inductance of

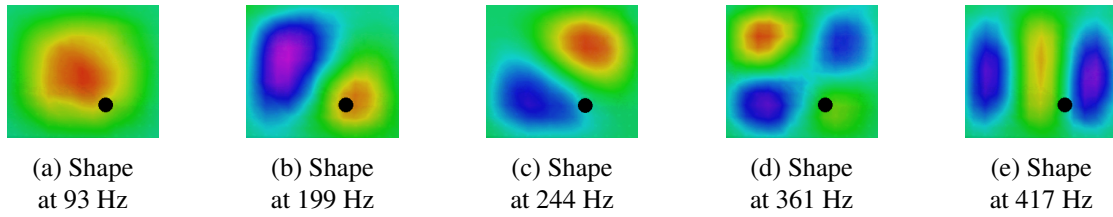


Figure 12: Measurement of five operational deflection shapes of the plate when a 207 g mass (in black) is added

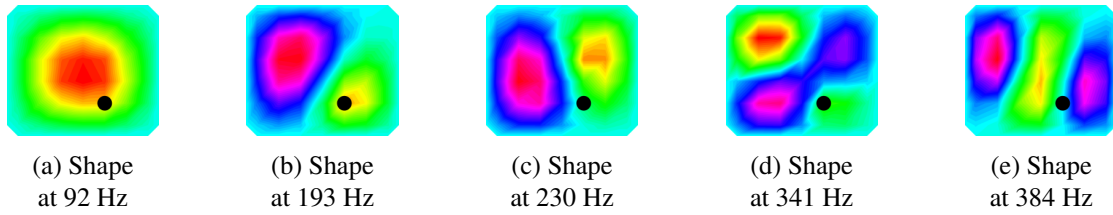


Figure 13: Measurement of five operational electrical current shapes in the network when a 1.34 H inductance (in black) replaces a 244 mH inductance of the network

244 mH should be replaced by an inductance of 1.34 H.

As previously explained in section 2.3, one way to validate the non-periodic plate electrical analogue is to compare the mechanical and electrical operational shapes. The measurements are still made with the setups presented in Figures 7 and 5. The results are shown in Figures 12 and 13. Since the plotted shapes look alike, we consider that the non-periodic network is the electrical analogue of the modified structure.

4.2 Multimodal vibration damping

The non-periodic plate is now coupled to its passive electrical analogue. The FRF measurement is made with the same setup as described in section 3.3. As seen in Figure 10, broadband damping is achieved in this case as well. This result validates the approach of coupling a non-periodic structure to its fully passive electrical analogue for multimodal damping purposes.

Moreover, the simulated results fit rather well with the measured ones. The remaining differences are due to the differences already spotted in Figure 11, and hence could be reduced by modelling the structural damping. As it is, it seems that the finite element model developed in this work can be used to predict the dynamics of a complex structure coupled to its electrical analogue. It could also be used to forecast where resistive components could be added in the network to improve the damping performance.

5 CONCLUSION

The first objective of this work is to develop a finite element model of a structure coupled to an electrical network interconnecting piezoelectric transducers. A structure covered with thin piezoelectric patches is considered. The electrical network is viewed as a passive controller that commands a relationship between the voltages and the charges on the upper electrodes of the piezoelectric transducers. The numerical results show a good agreement with measurements, even though the model could be improved. In the case here studied, the possible improvements include taking into account the structural damping

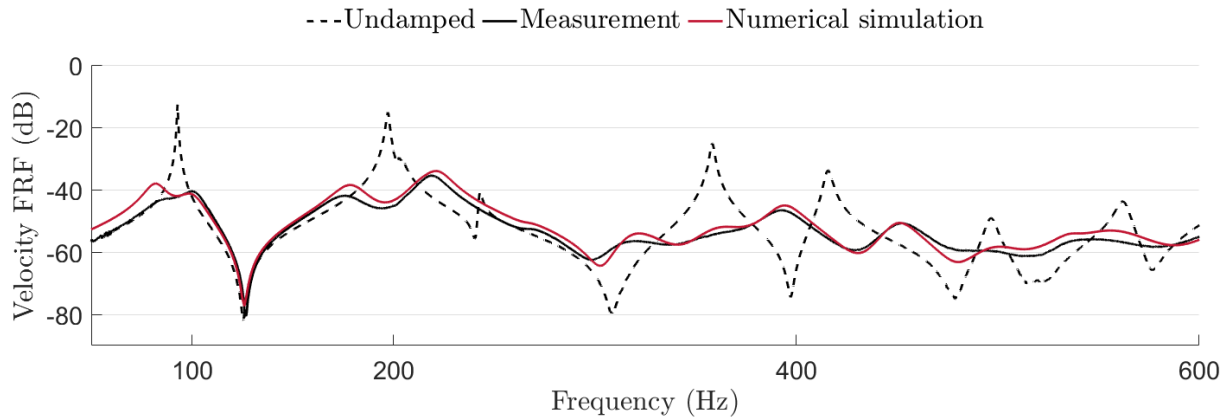


Figure 14: Experimental and simulated FRFs when the non-periodic plate is coupled to its electrical analogue

of the plate and the non-ideal boundary conditions of the setup. Anyway, the actual model can predict the dynamics of the coupled system. It could also be used to validate the analogy between a mechanical structure and its electrical analogue.

The other objective of this work is to extend to non-periodic structures the concept of coupling to an electrical analogue for passive multimodal damping purposes. To do that, the electrical analogue of a simply-supported plate is designed and its dynamics is experimentally validated. Finally, we measure the damping performance that is attainable by connecting the plate electrical analogue to the structure. These steps are repeated in the case of a plate on which a mass has been added in order to make it non-periodic. The final measurements highlight the achievable damping performance with a fully passive electrical network connected to the non-periodic structure. It is a first step towards trying to couple a complex structure to its electrical analogue for multimodal damping purposes.

REFERENCES

- [1] N. W. Hagood, A. Von Flotow, Damping of structural vibrations with piezoelectric materials and passive electrical networks, *Journal of Sound and Vibration* 146 (2) (1991) 243–268. doi : 10.1016/0022-460x(91)90762-9.
- [2] S. Behrens, S. O. R. Moheimani, A. J. Fleming, Multiple mode current flowing passive piezoelectric shunt controller, *Journal of Sound and Vibration* 266 (5) (2003) 929–942. doi : 10.1016/s0022-460x(02)01380-9.
- [3] M. Berardengo, S. Manzoni, A. M. Conti, Multi-mode passive piezoelectric shunt damping by means of matrix inequalities, *Journal of Sound and Vibration* 405 (2017) 287–305. doi : 10.1016/j.jsv.2017.06.002.
- [4] J. Ducarne, O. Thomas, J.-F. Deü, Placement and dimension optimization of shunted piezoelectric patches for vibration reduction, *Journal of Sound and Vibration* 331 (14) (2012) 3286–3303. doi : 10.1016/j.jsv.2012.03.002.
- [5] S. Vidoli, F. dell’Isola, Modal coupling in one-dimensional electromechanical structured continua, *Acta Mechanica* 141 (1-2) (2000) 37–50. doi : 10.1007/bf01176806.

- [6] R. H. MacNeal, The solution of partial differential equations by means of electrical networks, Ph.D. thesis, California Institute of Technology (1949).
- [7] S. U. Benscoter, R. H. MacNeal, Equivalent-plate theory for a straight multicell wing, NACA Technical Note 2786.
- [8] S. Alessandroni, F. dell'Isola, M. Porfiri, A revival of electric analogs for vibrating mechanical systems aimed to their efficient control by PZT actuators, *International Journal of Solids and Structures* 39 (20) (2002) 5295–5324. doi : 10.1016/s0020-7683(02)00402-x.
- [9] S. Alessandroni, U. Andreaus, F. dell'Isola, M. Porfiri, Piezo-ElectroMechanical (PEM) kirchhoff-love plates, *European Journal of Mechanics - A/Solids* 23 (4) (2004) 689–702. doi : 10.1016/j.euromechsol.2004.03.003.
- [10] S. Alessandroni, U. Andreaus, F. dell'Isola, M. Porfiri, A passive electric controller for multimodal vibrations of thin plates, *Computers & Structures* 83 (15-16) (2005) 1236–1250. doi : 10.1016/j.compstruc.2004.08.028.
- [11] B. Lossouarn, J.-F. Deü, M. Aucejo, K. A. Cunefare, Multimodal vibration damping of a plate by piezoelectric coupling to its analogous electrical network, *Smart Materials and Structures* 25 (11) (2016) 115042. doi : 10.1088/0964-1726/25/11/115042.
- [12] B. Lossouarn, M. Aucejo, J.-F. Deü, K. A. Cunefare, Design of a passive electrical analogue for piezoelectric damping of a plate, *Journal of Intelligent Material Systems and Structures* (2017) 1045389X1773123doi : 10.1177/1045389x17731232.
- [13] O. Thomas, J.-F. Deü, J. Ducarne, Vibrations of an elastic structure with shunted piezoelectric patches: efficient finite element formulation and electromechanical coupling coefficients, *International Journal for Numerical Methods in Engineering* 80 (2) (2009) 235–268. doi : 10.1002/nme.2632.
- [14] S. P. Timoshenko, S. Woinowsky-Krieger, *Theory of plates and shells*, McGraw-Hill, 1959.
- [15] A. Bloch, Electromechanical analogies and their use for the analysis of mechanical and electromechanical systems, *Journal of the Institution of Electrical Engineers - Part I: General* 92 (52) (1945) 157–169. doi : 10.1049/ji-1.1945.0039.
- [16] B. Lossouarn, M. Aucejo, J.-F. Deü, B. Multon, Design of inductors with high inductance values for resonant piezoelectric damping, *Sensors and Actuators A: Physical* 259 (2017) 68–76. doi : 10.1016/j.sna.2017.03.030.
- [17] O. Robin, J.-D. Chazot, R. Boulandet, M. Michau, A. Berry, N. Atalla, A plane and thin panel with representative simply supported boundary conditions for laboratory vibroacoustic tests, *Acta Acustica united with Acustica* 102 (1) (2016) 170–182. doi : 10.3813/aaa.918934.
- [18] A. J. Fleming, S. Behrens, S. O. R. Moheimani, Reducing the inductance requirements of piezoelectric shunt damping systems, *Smart Materials and Structures* 12 (1) (2003) 57–64. doi : 10.1088/0964-1726/12/1/307.